ACS Sustainable Chemistry & Engineering

Research Article

Cite This: ACS Sustainable Chem. Eng. 2019, 7, 20013−20021

pubs.acs.org/journal/ascecg

Preparation of MWCNTs-Graphene-Cellulose Fiber with Ionic Liquids

Yanrong Liu,[†,‡] Yanlei Wang,[†] Yi Nie,[*,†,§] Chenlu Wang,[†] Xiaoyan Ji,[‡] Le Zhou,[†] Fengjiao Pan,[†] and Suojiang Zhang[*,†]

[†]CAS Key Laboratory of Green Process and Engineering, Beijing Key Laboratory of Ionic Liquids Clean Process, State Key Laboratory of Multiphase Complex Systems, Institute of Process Engineering, Chinese Academy of Sciences, 1 North Second Street, Zhongguancun, Haidian District, 100190 Beijing, People's Republic of China

[‡]Energy Engineering, Division of Energy Science, Luleå University of Technology, Universitetsområdet Porsön, 97187 Luleå, Sweden

[§]Zhengzhou Institute of Emerging Industrial Technology, Yangjin Road, Jinshui District, 450000 Zhengzhou, People's Republic of China

ABSTRACT: The conductive multiwalled carbon nanotubes (MWCNTs)-graphene sheets (rGOs)-cellulose fiber was prepared with an eco-friendly wet-spinning method in which ionic liquid (IL) was used as both green solvent and dispersant. It was found that the selected IL 1-ethyl-3-methylimidazolium diethyl phosphate (EmimDep) shows remarkable capacities for dissolving cellulose and dispersing MWCNTs, and the synergistic effect of MWCNTs, rGOs, and cellulose results in a high electrical conductivity of 1195 S/m of MWCNTs-rGOs-cellulose fibers. Macropores and the double-layer structure of MWCNTs and rGOs can be observed by SEM in the studied fibers, and the number of macropores decreased with increasing rGOs amount, which is consistent with the result of the specific surface area. In addition, the prepared MWCNTs-rGOs-cellulose fibers present a nearly perfect electrical double-layer structure. The MWCNTs-rGOs-cellulose fiber with a mass ratio of 2:3:1 shows the best performance as the electrode candidate, with an electrical conductivity of 1195 S/m, specific capacitance of 597 mF/cm^2, and specific surface area of 91 m^2/g. Furthermore, the results from the molecular dynamics (MD) simulation evidenced that EmimDep can disperse CNTs effectively at 363.15 K, 1 atm compared to rGOs; the synergy effect of CNT and rGO exhibit great potential to enhance the dispersion than each individual component.

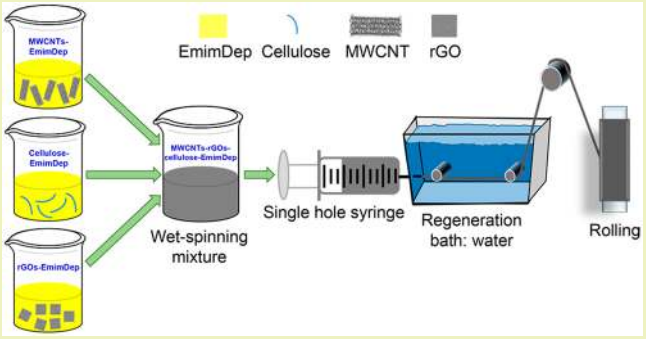

KEYWORDS: *Conductive cellulose fiber, Carbon nanotubes, Graphene, Ionic liquids, Wet spinning, Molecular dynamic simulation*

INTRODUCTION

Conductive fibers, consisting of polymer substrates and electrical conductors, have stirred up burgeoning interest for applications as an electronic device, a capacitor electrode, a neural probe, a biosensor and bioactuator, adsorption and absorption matrix, etc.[1−3] Cellulose, as the most abundant natural polymer in nature, has merits of biocompatibility, biodegradability, as well as high thermal and chemical stability.[4] Cellulose can be converted into conductive fibers by mingling with metal powders, carbon nanomaterials, or conductive polymers, among which cellulose-based carbon nanotubes (CNTs) and graphene (rGO, i.e., reduced graphene oxide) are the most intriguing conductive fibers due to their unique properties of biodegradability, lightweight, large surface area, and superior conductivity and capacitance.[5] Even though the hybrid materials of cellulose with CNTs and rGO exhibit great potential to improve the electrical, thermal, and electrochemical properties compared to each of the single components,[6] the limited research shows that the dispersion of CNTs and rGO as well as the dissolution of cellulose are two major problems in order to prepare CNTs-rGO-cellulose fibers.[7]

CNTs and rGO are easy to entangle together in water and the common organic solvents because of the strong van der Waals force, while cellulose is insoluble in these solvents due to the multiple H bonds among the cellulose molecules forming highly ordered crystalline regions.[8] Several solvents have been developed for the fabrication of CNTs- and/or rGO-cellulose compositions, such as acetone/*N*,*N*-dimethylacetamide (DMAc),[9] *N*-methylmorpholine oxide (NMMO),[10] and NaOH/urea solution.[11] However, these solvents in general have the drawbacks of volatility, toxicity, and difficulty in solvent recovery, calling for developing green solvents for CNTs and rGO dispersion and cellulose dissolution.

Ionic liquids (ILs) can be considered green solvents combining with their other remarkable properties such as

Received: September 26, 2019
Revised: November 14, 2019
Published: November 25, 2019

DOI: 10.1021/acssuschemeng.9b05489
ACS Sustainable Chem. Eng. 2019, 7, 20013−20021

Scheme 1. Wet-Spinning Procedure of MWCNTs-rGOs-Cellulose Fiber

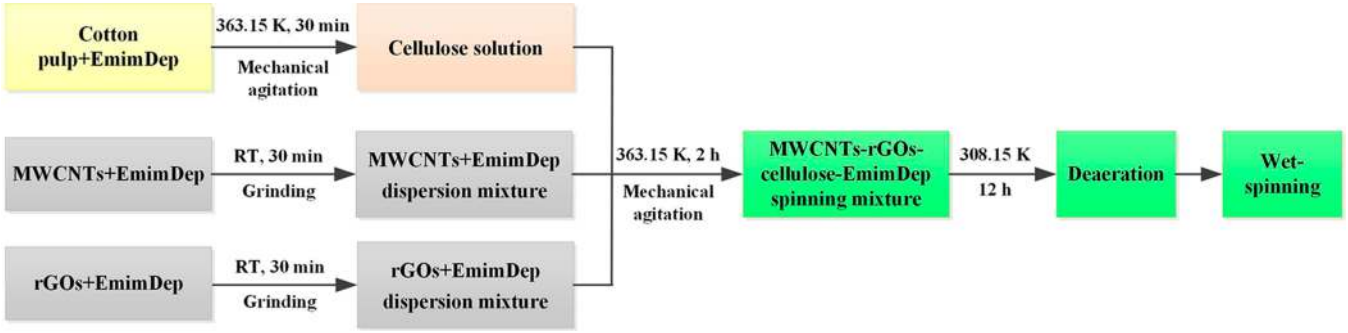

immeasurably low vapor pressure, excellent chemical and thermal stability, electrical conductivity, and nonflammability. ILs have received increasing attention.[12−15] Research has shown that ILs are capable of dispersing CNTs through noncovalent cation−π interactions to prevent their entanglement and dissolving cellulose at low temperatures.[16] It was reported that the suspension concentrations of single-walled carbon nanotubes (SWCNTs) dispersed by 1-hexadecyl-3-vinylimidazolium bromide (HvimiBr, IL) are enhanced by at least 20% with respect to the commonly used dispersants, such as sodium dodecyl sulfate, sodium dodecyl benzenesulfonate, and cetyltrimethylammonium bromide.[17] More importantly, ILs can act as a binder between CNTs and cellulose.[16] In addition, Bordes et al. evidenced that rGO could disperse and be stable in imidazolium-, pyrrolidinium-, and ammonium-based ILs;[18] Javed et al.[19] observed that rGO was uniformly incorporated into the hybrid cellulose fiber when using 1-butyl-3-methylimidazolium chloride (BmimCl) as a solvent. All of these imply that IL can be a promising candidate for fabricating CNTs-rGO-cellulose fibers.

Several studies of using ILs to produce CNTs- and/or rGO-cellulose conductive fibers have been reported. Javed et al.[19] developed a rGO-cellulose fiber with an electrical conductivity of 5.3×10^{-2} S/m using BmimCl as a solvent. Zhang et al.[20] investigated MWCNTs-cellulose fiber using 1-allyl-3-methylimidazolium chloride (AmimCl) as a solvent, and the fiber containing 4 wt % MWCNTs has an electrical conductivity of 0.83 S/m. 1-Ethyl-3-methylimidazolium acetate (EmimAc) was used as a solvent to fabricate MWCNTs-cellulose fiber,[21] achieving an electrical conductivity of 19 S/m for the sample with 0.07 wt % MWCNTs. For comparison, the MWCNTs-cellulose fiber fabricated from the organic solvent of NMMO has an electrical conductivity of 8.8×10^{-3} S/m for those containing 5 wt % MWCNTs.[22] The much higher electrical conductivity of IL-dispersed MWCNTs-cellulose fiber demonstrates that the dispersion of MWCNTs in the cellulose matrices is more effective when IL is used as solvent. In our previous work, the properties of wet spinning MWCNTs-cellulose fiber with a mass ratio of 5:1, spinning extrusion flow of 1 mL/min, and spinneret diameter of 0.46 mm was investigated using 1-ethyl-3-methylimidazolium diethyl phosphate (EmimDep) as the solvent,[23] and 760 S/m electrical conductivities and 187 m^2/g specific surface area were observed for the studied MWCNTs-cellulose fiber. These results evidenced that EmimDep can be a potential solvent to disperse MWCNTs and dissolve cellulose. However, to the best of our knowledge, the investigation of ILs for the preparation of CNTs-rGO-cellulose fibers has not been studied sufficiently. In addition, some attempts have been made to prepare lithium-ion batteries and electrochemical supercapacitors based on CNTs or rGO fibers, and both high electrical conductivity and electroactivity are required for these electronic devices. However, these properties cannot be simultaneously achieved with either CNTs or rGO fibers.[24]

According to our previous study, the MWCNTs-cellulose fiber with a mass ratio of 5:1 has the highest electrical conductivity, surface area, and specific volumetric capacitance compared to those with ratios of 2:1, 3:1, and 4:1.[23] Therefore, a constant mass ratio of (MWCNTs+rGOs):cellulose (i.e., 5:1) was selected for further study in this work. The aim of this work was to fabricate novel MWCNTs-rGOs-cellulose fibers with an eco-friendly wet-spinning process using EmimDep as a green solvent and dispersant. The effects of the MWCNTs, rGOs, and cellulose mass ratios of 5:0:1, 4:1:1, 3:2:1, 2:3:1, and 1:4:1 on the fiber characteristics were investigated via electrical conductivity, electrochemical properties (i.e., cyclic voltammetry and specific capacitance), and specific surface area. The surface morphologies of the original material and the fabricated MWCNTs-rGOs-cellulose fiber were characterized with SEM, and the synergistic effects on the dispersion of CNTs and rGOs in EmimDep were further illustrated by conducting molecular dynamics (MD) simulations with different temperatures.

EXPERIMENTAL SECTION

Materials. The MWCNTs (>98 wt %) was purchased from Cnano Technology (Zhenjiang) Ltd. with a length of <10 μm and diameter of 10−15 nm. rGOs was synthesized based on the modified Hummers method.[25] Cellulose (cotton pulp) was provided by Henan Dingda Biological Technology Co. Ltd. EmimDep (>99 wt %) was synthesized in the lab, and the synthetic procedure and characterization were described in detail in our previous work.[26,27]

Fiber Manufacture Procedures. The procedures for preparing the MWCNTs-rGOs-cellulose fibers with difference mass ratios are described as follows.

(1) Cotton pulp (0.1 g) with EmimDep (10 g) was heated in a thermostatic oil bath at 363.15 K by mechanical mixing for 30 min to obtain a clear 1 wt % cellulose solution.

(2) Five MWCNTs-rGOs mixtures (0.5 g) with difference mass ratios (MWCNTs:rGOs = 5:0, 4:1, 3:2, 2:3, and 1:4) were suspended into EmimDep (10 g). Afterward, the obtained mixtures were further ground in an agate mortar for 30 min at room temperature (RT) to obtain homogeneous mixtures. Each of the five mixtures was added into the 1 wt % cellulose solution at 363.15 K and treated with mechanical mixing for 2 h to acquire five homogeneous spinning mixtures.

(3) The obtained spinning mixtures in step 2 was placed in a vacuum drying oven to deaerate at 308.15 K for 12 h before use.

(4) After deaeration, each spinning mixture was transferred into a syringe. The syringe was fixed into lab-built wet-spinning equipment, which consisted of a syringe pump, a regeneration bath (water is coagulation), and a winding shift. The above-

DOI: 10.1021/acssuschemeng.9b05489
ACS Sustainable Chem. Eng. 2019, 7, 20013−20021

mentioned spinning mixtures were spun into the water regeneration bath directly at room temperature with an extrusion flow of 1.0 mL/min through a single-hole spinneret needle of 0.98 mm with no winding. The length−diameter ratio of the spinneret needle was set to be 2 as suggested by Hauru et al.[28] to obtain a better strength property for cellulose spinning.

(5) After wet spinning, the wet fibers were soaked in deionized water and washed 5 times to remove EmimDep.[29] Then the washed wet fibers were rolled at room temperature and sent to a vacuum drying oven at 308.15 K for 48 h to remove water. The dried MWCNTs-rGOs-cellulose fibers with different mass ratios of 5:0:1. 4:1:1, 3:2:1, 2:3:1, and 1:4:1 were further characterized.

The wet-spinning procedure of MWCNTs-rGOs-cellulose fiber is summarized in Scheme 1.

Experimental Apparatus and Procedure. *Electrical Conductivity.* The electrical conductivities of pure MWCNTs and rGOs were measured with the methods reported by Song et al.[30] and Marinho et al.,[31] respectively. The MWCNTs were mixed with poly(vinylidene fluoride) (PVDF) uniformly at a mass ratio of 1:1 and put into a tablet press (HF-2A) to prepare the film at a pressure of 15 MPa. The electrical conductivities of the prepared MWCNTs film and rGOs were measured with an impedance analyzer (RTS-9) based on the four-probe method, each sample was repeated for 3 times, and the average value was reported.

The electrical conductivity of MWCNTs-rGOs-cellulose fiber was measured by a two-probe method. The resistance (R) of the obtained fiber was measured (3 times) by a precision voltmeter (LINI-T, UT58A). The volume resistivity ρ of the fiber was calculated by taking into account the section area (A) and the length (L) of the fiber between the contacts: $\rho = R \times A/L$. Then the electrical conductivity γ (S/m) of the fiber was acquired from the reciprocal of the resistivity, i.e., $\gamma = L/(R \times A)$.[32,33]

Tensile Strength. The mechanical properties of the MWCNTs-rGOs-cellulose fibers were measured by a Dynamic Mechanical Analyzer (DMA Q800) at 30 °C with a rate force and upper force limit of 0.05 N/min and 18 N, respectively.[34]

Scanning Electron Microscopy (SEM). The acquired fibers were characterized by SEM (SU8000, Japan, 5.0 kV). The sample was sputtered with platinum for better observation using a JEC-3000FC auto fine coater. The current and sputtering time were set to be 20 mA and 30 s, respectively.

Electrochemical Property. The electrochemical property of cyclic voltammetry (CV) was characterized using a cell with three electrodes: a working electrode (MWCNTs-rGOs-Cellulose fiber), a counter electrode (Pt filament), and a reference electrode (Ag filament). The electrode was immersed into aqueous NaCl (0.1 M) and connected to an electrochemical workstation (CH Instruments, model CHI660E). The length of the electrode that was immersed in NaCl aqueous solution was about 1 cm. CV measurement was performed from 0 to 0.4 V at a 10 mV/s scan rate. The specific capacitance of the MWCNTs-rGOs-cellulose fiber in the cell was determined according to the method of Yu et al.[35]

Specific Surface Area. The specific surface area of the fabricated fiber was determined from nitrogen physisorption measurement at liquid-nitrogen temperature on a Micromeritics ASAP 2460 instrument (Micromeritics, Norcross, GA, USA).

COMPUTATIONAL SECTION

All of the simulations in this work were accomplished using a large-scale atomic/molecular massively parallel simulator (LAMMPS).[36] The time step for integrating Newtonian equations of motion was set to be 2 fs to guarantee energy conservation. The all-atom-optimized potential for the liquid simulations (OPLS-AA) was taken for MWCNTs and rGO,[37] and this method has been used successfully to predict the structural and mechanical properties of MWCNTs and rGO.[38] For EmimDep, the parameters of the bond, angle, dihedral, van der Waals interactions, and electrostatic interactions were described by the OPLS-AA[39] force field that has been used successfully to capture the structures and liquid properties of ILs.[30−43] The interactions between the IL and the rGO include both electrostatic and van der Waals terms. The former term, i.e., the long-range Coulombic interaction, was computed using the particle−particle−particle−mesh (PPPM) algorithm,[44] and the later one was described via the 12−6 Lennard−Jones potential. The Lorentz−Berthelot mixing rules were used to model the parameters truncated at 1.2 nm for the mixture of EmimDep and rGO.

To analyze the structures and dispersion properties of MWCNTs and rGOs in EmimDep as well as the synergistic dispersion effect of MWCNTs and rGOs in EmimDep, three hybrid systems were constructed. The first system is composed of a 4.12 nm long and 4.06 nm width AB-stacked bilayer rGOs (ABBrGOs) with an interlayer distance of 0.34 nm inserted into a $8.1 \times 8.1 \times 4.9$ nm^3 box with 800 pairs of EmimDep. For the second system, we inserted two double-well-CNTs (DWCNTs) with a distance of 0.36 nm into the box of 1000 pairs of EmimDep to compose the second box, the chiral index for these two inner tubes is set to be (5,5), and the second box size is $7.4 \times 7.4 \times 7.4$ nm^3. The third system is composed of DWCNT and ABBrGO with a distance of 0.35 nm into a $8.8 \times 8.8 \times 5.3$ nm^3 box with 1000 pairs of EmimDep. A periodic boundary condition (PBC) was applied in the x, y, and z directions of each box. In the MD simulations, EmimDep, DWCNTs, and ABBrGOs were relaxed in a NPT ensemble for 1 ns with a temperature of 300 K and a pressure of 1 atm along x, y, and z directions using temperature and barostat coupling constants of 0.2 and 2 ps, respectively. After the system reached equilibrium, the temperature of the system was raised from 300 to 363.15 K in the NPT ensemble at a pressure of 1 atm. When the temperature of the system was increased to 363.15 K, MD simulations continued to run an additional 10 ns in the NPT ensemble at 363.15 K and 1 atm in order to collect data for analyzing. To further study the impact of temperature, after the system reached equilibrium, the system temperature was raised from 363.15 to 500 K to repeat the MD simulations but with an additional 2 ns.

RESULTS AND DISCUSSION

Experimental Results. In order to study the effects of the ratios of MWCNTs, rGOs, and cellulose on the fiber properties, MWCNTs-rGOs-cellulose fibers (5:0:1, 4:1:1, 3:2:1, 2:3:1, 1:4:1) were prepared.

The electrical conductivities of pure MWCNTs and rGOs as well as those for the fibers are presented in Figure 1, in which the electrical conductivity of the SWCNTs-rGOs-cellulose fiber with a mass ratio of 1:4:0 was cited from Yu et al.[35] for comparison. As shown in Figure 1, the electrical conductivity of MWCNTs studied in this work is 28.8 S/m, which is within the range of those for the CNTs studied by Ebbesen et al.[45] Ebbesen

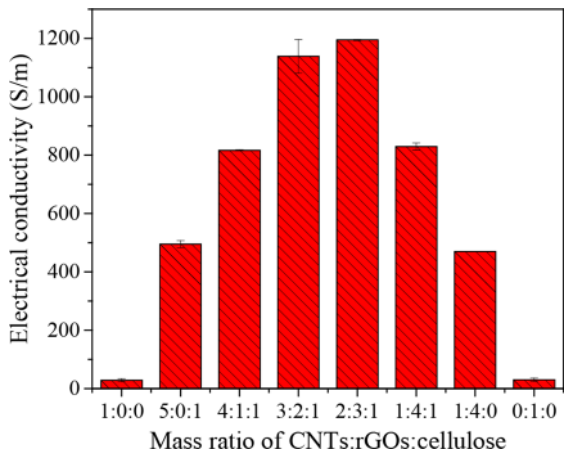

Figure 1. Electrical conductivities of MWCNTs, rGOs, and CNTs-rGOs-cellulose fibers with different amounts of CNTs and rGOs. CNT type with ratios of 1:0:0, 5:0:1,[23] 4:1:1, 3:2:1, 2:3:1, and 1:4:1 represent MWCNTs, while that with a ratio of 1:4:0 represents SWCNTs.[35]

DOI: 10.1021/acssuschemeng.9b05489
ACS Sustainable Chem. Eng. 2019, 7, 20013−20021

et al. investigated the electrical conductivity for eight types of CNTs with the same four-probe method, and their electrical conductivities were reported in a range of 1.7−2.0 × 10^6 S/m, depending on the length−radius ratio of CNTs. The electrical conductivity of rGOs is 30.4 S/m, which is slightly higher than those for the MWCNTs studied in this work. According to the study by Marinho et al., the electrical conductivities of the compacted MWCNTs and rGOs depend on the mechanical particle arrangement and deformation mechanisms.[31] In this study, the electrical conductivities of the compacted rGOs are from tens to 262 S/m at compacted pressures of 0−5 MPa.

After dispersing MWCNTs and dissolving cellulose in EmimDep, the electrical conductivity of the prepared MWCNTs-rGOs-cellulose at a mass ratio of 5:0:1 (495 S/m) is significantly increased (17 times) compared to that of MWCNTs, indicating that EmimDep is an efficient solvent for the MWCNTs dispersion and cellulose dissolution.[26,34] Salazar et al. evidenced that the imidazolium-based ILs have a higher dispersion capability than the organic solvent for MWCNTs.[46] The electrical conductivity of MWCNTs can be improved 3−5 times in 1-butyl-3-methylimidazolium hexafluorophosphate ($BmimPF_6$), 1-butyl-3-methylimidazoliumhydrogensulfate ($BmimHSO_4$), and 1-methyl-3-propylimidazolium iodide (PmimI) due to the weak van der Waals interactions between the imidazolium cations and the MWCNT walls. Krainoi et al. indicated that the electrical conductivity of MWCNTs-rubber can be improved more than 10 times by 1-butyl-3-methyl imidazolium bis(trifluoromethylsulfonyl)mide (BmimTFSI) due to a good dispersion of MWCNTs,[47] which supports our results.

With increasing the content of rGOs in MWNTs-rGOs-cellulose fiber (Figure 1), the electrical conductivity first increased and then decreased. As shown in Figure 1, the average electrical conductivity of CNTs-rGOs-cellulose (3:2:1) is 1138 S/m, while it is 1195 S/m for the MWCNTs-rGOs-cellulose (2:3:1), the one with the highest conductivity. This value is much higher than those for the MWCNTs-rGOs-cellulose (5:0:1) (495 S/m) and SWCNTs-rGOs-cellulose (1:4:0) (470 S/m). The electrical conductivity of MWCNTs is much lower compared to the perfect SWCNTs,[48] and it is more reasonable to use the electrical conductivity of 1:4:0 SWCNTs-rGOs-cellulose as a reference to evaluate the performance of the conductive fibers prepared in this work. The comparison shows a much higher value of electrical conductivity, indicating a more conductive path existed in the MWCNTs-rGOs-cellulose fibers.

A comparison of the results for the samples of MWCNTs-rGOs-cellulose at mass ratios of 1:4:1 and 5:0:1 as well as that for SWCNTs-rGOs-cellulose of 1:4:0 can reflect the effects of rGOs and cellulose on dispersing CNTs. The electrical conductivity of MWCNTs-rGOs-cellulose (1:4:1) with a value of 829 S/m is higher than that for the MWCNTs-rGOs-cellulose (5:0:1, 495 S/m). The MWCNTs dispersion for the case of rGOs-cellulose was better than that with cellulose only, reflecting the synergistic effect for rGOs and cellulose. Additionally, the electrical conductivity of MWCNTs-rGOs-cellulose (1:4:1) is higher than that of SWCNTs-rGOs-cellulose (1:4:0, 470 S/m), indicating that CNTs are dispersed more efficiently by cellulose than that by rGOs. Moreover, the electrical conductivities follow the order of MWCNTs-rGOs-cellulose (1:4:1) > MWCNTs-rGOs-cellulose (5:0:1) > SWCNTs-rGOs-cellulose (1:4:0), indicating MWCNTs are dispersed more uniformly by rGOs-cellulose, followed by cellulose and rGOs. This observation agrees with the results by Xu et al.[49] and Ioniţă et al.[50]

The mechanical property, i.e., the tensile strength, is displayed in Figure 2. As shown in Figure 2, the tensile strengths of

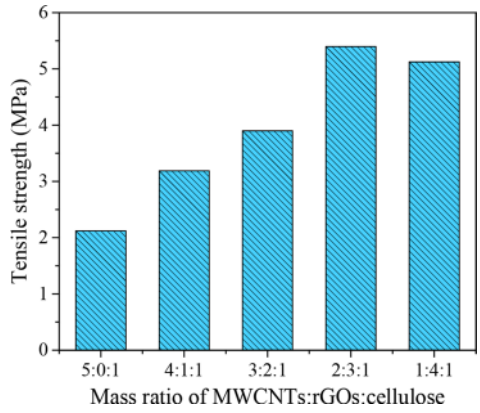

Figure 2. Tensile strength of MWCNTs-rGOs-cellulose fibers with different amounts of MWCNTs and rGOs in cellulose.

MWCNTs-rGOs-cellulose fibers with mass ratios of 4:1:1, 3:2:1, 2:3:1, and 1:4:1 were stronger than that with 5:0:1. One one hand, the stronger tensile strength was attributed to the better interfacial interaction between rGOs-cellulose and MWCNTs.[49] On the other hand, it also illustrated that MWCNTs were dispersed more uniformly by rGOs-cellulose than by cellulose, which agrees with the electrical conductivity result. Jiang et al. prepared the CNTs-rGOs-polyacrylonitrile (PAN) fibers in the 0.5% PAN solution, and their mechanical strength is in a range of 1.5−6.5 MPa,[51] consistent with the results in our study, i.e., 2.1−5.4 MPa. Even though the tensile strength of the prepared MWCNTs-rGOs-cellulose fiber is decreased with the addition of carbon nanomaterial in cellulose compared with the pure cellulose fiber,[23] it still has promising multifunctional applications as energy absorbers, mechanical sensors, and heat exchangers as reported by Jiang et al.[51]

Figure 3a−i shows the SEM morphologies of original materials and the studied fibers. The original MWCNTs (Figure 3a) presented a structure of irregularly aggregating and tangling together with each other, while the original rGOs possesses a lamellar structure (Figure 3b). For the original cellulose (i.e., cotton pulp), the folding feature was observed by SEM.

The SEM morphologies of MWCNTs-rGOs-cellulose (5:0:1) are depicted in Figure 3d and 3e. After dissolving the cellulose and dispersing the MWCNTs by EmimDep, the folding feature of the raw cellulose disappeared and a smooth-looking surface was observed (Figure 3d), indicating a good dissolution of the cellulose in EmimDep. In Figure 3e, MWCNTs dispersed uniformly instead of serious aggregation, and the regenerated cellulose was around the MWCNTs, which indicated that the MWCNTs were dispersed effectively by EmimDep and the cellulose.[19,24,48] The good dispersion of MWCNTs can be attributed to electrostatic repulsion of the interfacial interactions between the oxygen groups on the CNTs and the cellulose.[52] In addition, the macropores formed by the interlaced MWCNTs can be observed clearly in Figure 3e and 3g. As reported, these macropores can serve as reservoirs for gas adsorption[3] and ion buffering.[52]

When adding the MWCNTs and rGOs into the cellulose solution, as can be seen in Figure 3f and 3g, rGOs was inserted into the MWCNTs and cellulose and the MWCNTs were uniformly dispersed on the surface of rGOs to form a double-

DOI: 10.1021/acssuschemeng.9b05489
ACS Sustainable Chem. Eng. 2019, 7, 20013−20021

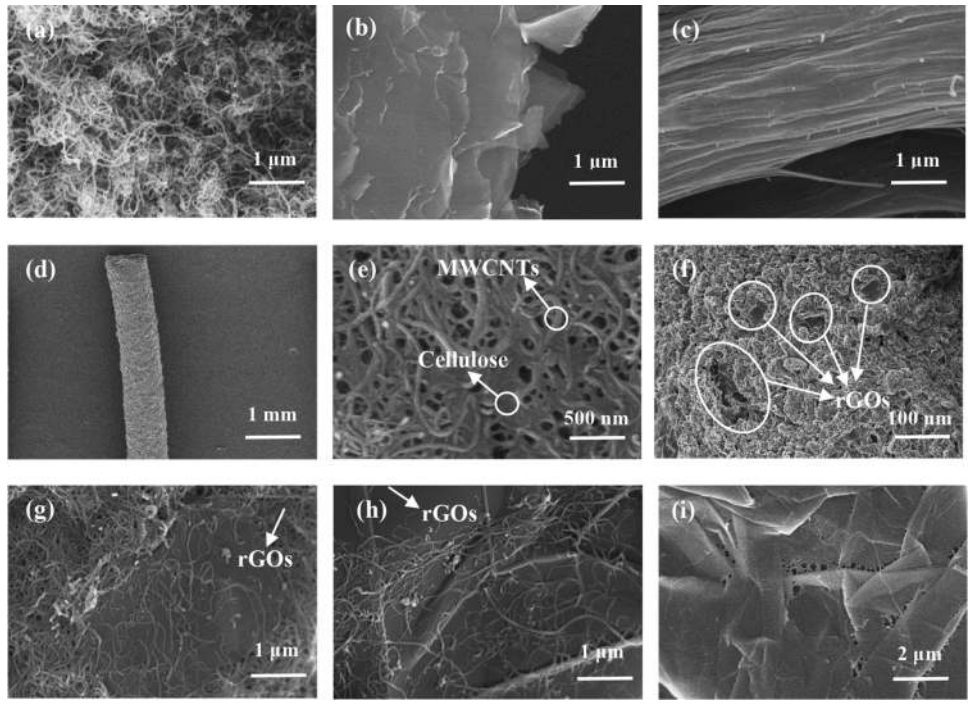

Figure 3. SEM of original materials and the fabricated fibers: (a) original MWCNTs, (b) original rGOs, (c) original cotton pulp, (d and e) 5:0:1 MWCNTs-rGOs-cellulose fiber, (f) 3:2:1 MWCNTs-rGOs-cellulose fiber, (g) 4:1:1 MWCNTs-rGOs-cellulose fiber, (h) 2:3:1 MWCNTs-rGOs-cellulose fiber, and (i) 1:4:1 MWCNTs-rGOs-cellulose fiber. Fiber spinning extrusion flow is 1 mL/min, and spinneret diameter is 0.98 mm.

layer structure. These illustrated that through the repulsion interaction between the cellulose and MWCNTs and the π-stacking effect between the MWCNTs and rGOs, the system could be better dispersed by the synergistic effect,[45] giving the material better performance, such as higher electrical conductivity. Moreover, with increasing the mass ratio of rGOs in the fiber, the double-layer structure of the MWCNTs and rGOs is more obvious under the same magnification (Figure 3h). When the mass ratio of rGOs in the MWCNTs and cellulose reached 4:1:1, the double layer became weak significantly compared to the 2:3:1 MWCNTs-rGOs-cellulose, leading to relatively low conductivity. Therefore, the double-layer structure is beneficial to the high electrical conductivity for the studied fiber.

The electrochemical properties of four MWCNTs-rGOs-cellulose fibers with higher electrical conductivities were further characterized with CV and specific capacitance. The CV analysis was conducted with a scan rate of 10 mV/s in the voltage window of from 0 to 0.4 V and 0.1 M NaCl solution. The results of CV are depicted in Figure 4, showing a high degree of electroactivity with near-ideal rectangular curves, a characteristic of an electrical double-layer structure. This result agrees with those from Ramesh et al.[53] and Lin et al.[54]

The integral area of the CV curve indicates the electrochemical capacitance of the MWCNTs-rGOs-cellulose fiber. According to the study by Yu et al.,[35] the specific capacitances were acquired as shown in Figure 5. With increasing the amount of rGOs in the fiber, the specific capacitances of the studied fibers increased from 313 to 709 mF/cm^2, implying that the specific capacitance largely depends on the amount of rGOs. Sun et al.[24] prepared supercapactiors using CNTs and CNTs-rGOs fibers as electrodes with specific capacitances up to 0.90 and 4.97 mF/cm^2, respectively. The capacitance of the studied MWCNTs-rGOs-cellulose fiber in this work is much higher

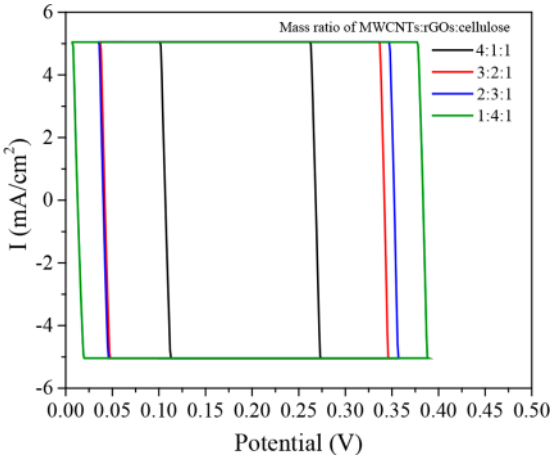

Figure 4. Cyclic voltammetry curves in aqueous NaCl 0.1 M with a scan rate of 10 mV/s for the MWCNTs-rGOs-cellulose fibers.

compared to those from Sun et al., indicating potential application of MWCNTs-rGOs-cellulose fiber in the electrochemical field. On the basis of the report, the electrical conductivity and electroactivity (i.e., specific capacitance) are two important properties for a potential electrochemical application, and the MWCNTs-rGOs-cellulose (2:3:1) fiber could be a better material in the application of electrochemical field.

The specific surface area of the prepared fibers is shown in Figure 6, revealing that the specific surface area is decreased greatly with the increase of rGOs amount. The possible reasons are ascribed to the fact that the low specific surface area of rGOs and the double-layer structure formed by MWCNTs and rGOs can effectively reduce the MWCNT interlacing, i.e., reducing the porosity. This explanation can be supported by the SEM study.

DOI: 10.1021/acssuschemeng.9b05489
ACS Sustainable Chem. Eng. 2019, 7, 20013−20021

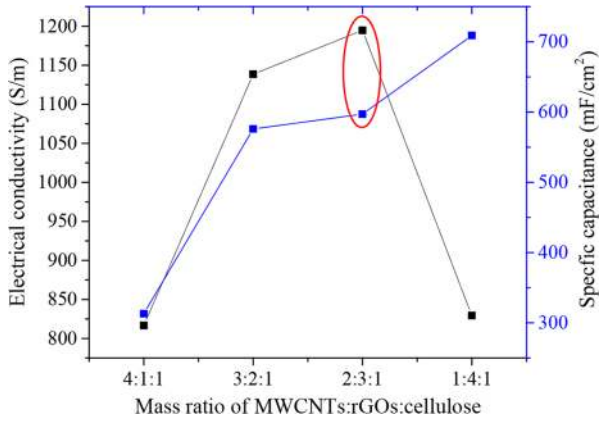

Figure 5. Effect of MWCNTs and rGOs on the electrical conductivity and specific capacitance.

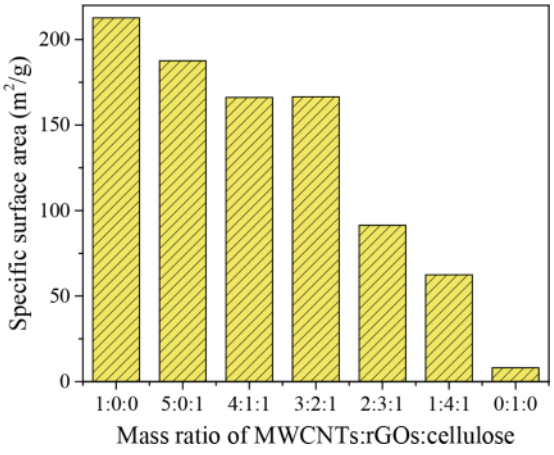

Figure 6. Surface area of MWCNTs, rGOs, and MWCNTs-rGOs-cellulose fibers with mass ratios of 5:0:1, 4:1:1, 3:2:1, 2:3:1, and 1:4:1.

As can be seen from Figure 3e and 3g–i, with increasing amount of rGOs in the fiber, the number of macropores is significantly reduced, resulting in a low specific surface area. According to the results shown in Figure 6, the specific surface area for the MWCNTs-rGOs-cellulose (5:0:1) is 188 m^2/g, while that for the MWCNTs-rGOs-celluloses (4:1:1 and 3:2:1) is around 167 m^2/g.

Compared with the previously reported surface areas of carbon microfiber (<10 m^2/g) and CNTs-coated carbon fiber (34.6 m^2/g),[55] dry-spun MWCNTs fiber (100 m^2/g),[56] as well as wet-spun SWCNTs fiber (160 m^2/g),[3] the prepared MWCNTs-rGOs-cellulose fibers with ratios of 5:0:1, 4:1:1, and 3:2:1 have larger specific surface areas. According to Neimark et al.,[3] the wet-spun SWCNTs fiber with a specific surface area of 160 m^2/g is capable of adsorbing gas and absorbing liquid effectively; therefore, the prepared MWCNT-rGOs-cellulose fibers can also be used as adsorption and absorption materials, e.g., for ion-buffering reservoirs.

Computational Results. MD simulation was performed to deeply understand the dispersion mechanism of the MWCNTs and rGOs in EmimDep. Figure 7a represents the atomic structure of EmimDep used in this work. The interaction energy of each conductive nanomaterial, denoted as ABBrGOs, DWCNTs, or DWCNT/ABBrGO, was calculated. As shown in Figure 7b, each of the interaction energies reaches balance under the simulation conditions of 363.15 K, 1 atm, and 10 ns. In addition, the dispersion behaviors were simulated for three different hybrid systems: (a) ABBrGOs/EmimDep, (b) DWCNTs/EmimDep, and (c) DWCNT/ABBrGO/EmimDep. The simulation results (Figures 8a–c) showed that these three systems could not be dispersed at 300 K, 1 atm, and 1 ns. After a longer time simulation (10 ns) in the NPT ensemble at 363.15 K and 1 atm, both DWCNTs (Figure 8e) and DWCNT/ABBrGO (Figure 8f) would be separated while ABBrGOs still maintained the initial configuration (Figure 8d). To detect the impact of temperature on the dispersion of nanomaterials in EmimDep, the simulations at 500 K and 1 atm were also performed (Figures 8g–i). The results illustrated that the dispersions of DWCNTs (Figure 8h) and DWCNT/ABBrGO (Figure 8i) are much better at 500 K than those at 300 and 363.15 K, evidencing that high temperature will promote the separation velocity of the hybrid nanomaterials.

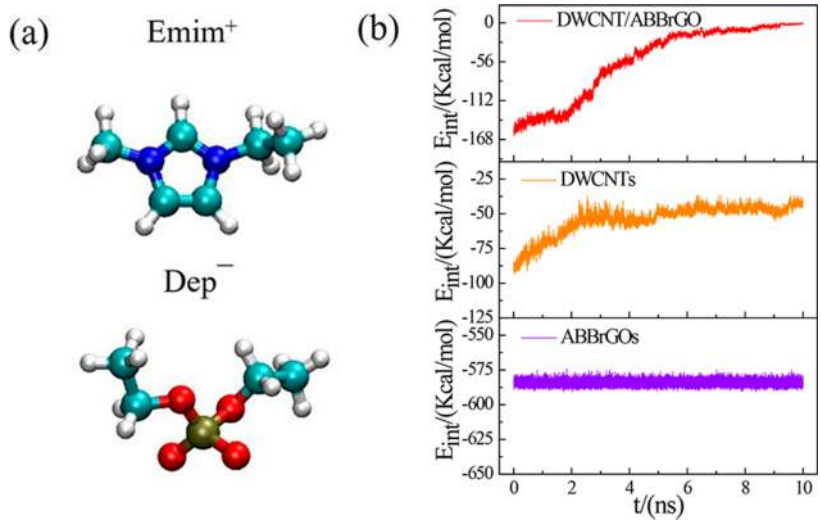

Figure 7. (a) Atomic structure of EmimDep considered in this work. (b) Interaction energy between two materials inserted into the three boxes of EmimDep, where the violet, orange, and red color represent the interaction energy between ABBrGOs, DWCNTs, and DWCNT/ABBrGO, respectively. For each box, all of the data were collected from a 10 ns MD simulation in the NPT ensemble at 363.15 K and 1 atm.

DOI: 10.1021/acssuschemeng.9b05489
ACS Sustainable Chem. Eng. 2019, 7, 20013–20021

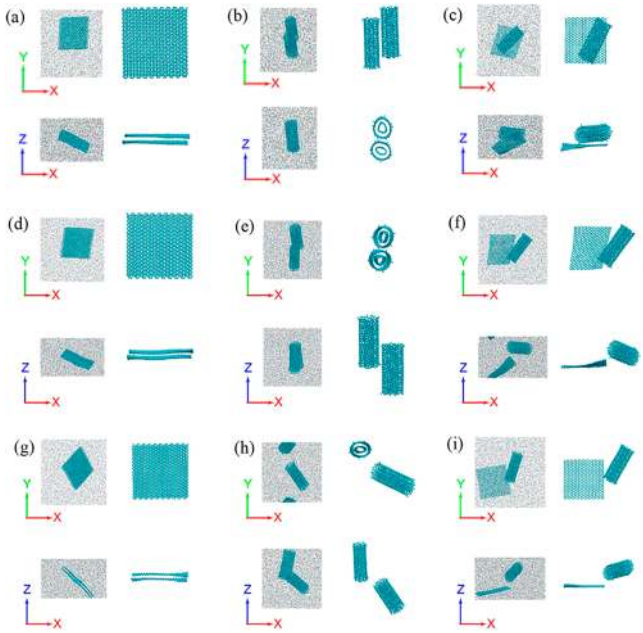

Figure 8. Simulation snapshots of three composed systems considered in this study, where the cyan color in three boxes represents ABBrGOs/EmimDep (a, d, g), DWCNTs/EmimDep (b, e, h), DWCNT/ABBrGO/EmimDep (c, f, i). Surrounding of each composed material is EmimDep. (a−c) Hybrid systems are the last snapshot of a 1 ns MD simulation in the NPT ensemble at 300 K and 1 atm; (d−f) hybrid systems are the last snapshot of a 10 ns MD simulation in the NPT ensemble at 363.15 K and 1 atm; (g−i) hybrid systems are the last snapshot of a 10 ns MD simulation in the NPT ensemble at 500 K and 1 atm.

In order to reveal the intrinsic mechanism, the total potential energy and inter potential energy are summarized in Figure 9a−c, showing that the total potential energy of DWCNTs (Figure 9b) and DWCNT/ABBrGO (Figure 9c) in EmimDep was decreased gradually. However, the total potential energy of ABBrGOs changes slightly, indicating that it might be difficult to use EmimDep to separate the graphene bilayer system (Figure 9a). From the inter potential energy, it can be observed that the dispersion potentials of these three systems follow the order DWCNT/ABBrGO/EmimDep > DWCNTs/EmimDep > ABBrGOs/EmimDep owing to a smaller contacting area of CNT compared to that of rGO[57] and the synergy effect of CNT and rGO. Atif et al.[57] reported that the volume fraction of the CNT and rGO also influences their dispersion state due to the larger volume fraction of rGO than CNT, making it very difficult to achieve a uniform dispersion beyond a certain volume fraction. Combined with the experimental results, we state that the excellent conductivity of MWCNTs-rGOs-cellulose fiber may be attributed to the good dispersion of MWCNTs in EmimDep and the synergistic effects of MWCNTs and rGOs.

CONCLUSION

In this work, the wet-spinning method was used for fabricating conductive MWCNTs-rGOs-cellulose fibers with mass ratios of 5:0:1, 4:1:1, 3:2:1, 2:3:1, and 1:4:1 where EmimDep was used as the green solvent and dispersant. The electrical conductivity, SEM, electrochemical properties, and specific surface area were applied in systemically studying the characteristics of the prepared fibers. It was found that the remarkable electrical conductivity is attributed to the good dispersion of MWCNTs in EmimDep and the synergistic effect of MWCNTs, rGOs, and cellulose, and the maximum electrical conductivity of 1195 S/m was obtained under a mass ratio of 2:3:1 of MWCNTs-rGOs-cellulose fiber. The specific surface area of the studied fiber decreased from 187.6 to 62 m^2/g with increasing rGOs amount, which agreed with the SEM result, i.e., the observed macropores in the studied fiber decreased with increasing rGOs amount. The CV curve result illustrated that a nearly perfect electrical double-layer structure formed with a high degree of electroactivity for four selected MWCNTs-rGOs-cellulose fibers (4:1:1, 3:2:1, 2:3:1, and 1:4:1). The calculated specific capacitance from the CV result increased from 313 to 709 mF/cm^2 with increasing rGOs in the fiber, indicating that the specific capacitance largely depends on the performance of rGOs. Because of the potential application of MWCNTs-rGOs-cellulose fiber electrode depending on both the high electrical conductivity and the specific capacitance, the MWCNTs-rGOs-cellulose fiber with a mass ratio of 2:3:1 and electrical conductivity of 1195 S/m, specific capacitance of 597 mF/cm^2, and specific surface area of 91 m^2/g was supported to be the best one as the electrode candidate. In addition, the MD results evidenced that EmimDep can significantly disperse MWCNTs at 363.15 K, 1 atm, compared with rGOs, and the synergy effect of CNTs and rGOs can enhance the dispersion. When increasing the dispersion temperature from 363.15 to 500 K, the dispersions of CNTs and rGOs are more obvious, indicating that increasing the temperature will promote the separation velocity of the MWCNTs and rGOs.

AUTHOR INFORMATION

Corresponding Authors

*E-mail: ynie@ipe.ac.cn. Phone: +86-10-82844875.
*E-mail: sjzhang@ipe.ac.cn. Phone: +86-10-82627080.

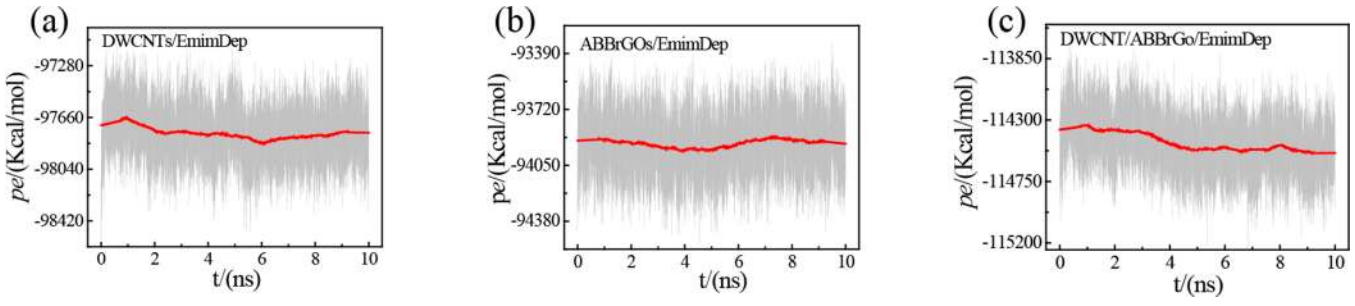

Figure 9. (a−c) Potential energy of the entire system for three cases considered in this study, where the gray and red colors represent initial data and averaged data, respectively. For each case, all of the initial data are collected from a 10 ns MD simulation in the NPT ensemble at 363.15 K and 1 atm.

DOI: 10.1021/acssuschemeng.9b05489
ACS Sustainable Chem. Eng. 2019, 7, 20013−20021

ORCID

Yanlei Wang: 0000-0002-2214-8781
Yi Nie: 0000-0002-4111-6136
Le Zhou: 0000-0002-9647-7924
Suojiang Zhang: 0000-0002-9397-954X

Notes

The authors declare no competing financial interest.

■ ACKNOWLEDGMENTS

This work was supported by National Natural Science Foundation of China (Grant Nos. 21776276, 21576262, 21890762, and 21808220), Beijing Municipal Natural Science Foundation (2182070), and Zhengzhou High Level Talent (20180300045). Y.L. and X.J. are also thankful for financial supports from the Carl Tryggers Stiftelse and Kempe Foundations.

■ REFERENCES

(1) Hao, X. D.; Wang, J.; Ding, B.; Wang, Y.; Chang, Z.; Dou, H.; Zhang, X. G. Bacterial-cellulose-derived interconnected meso-microporous carbon nanofiber networks as binder-free electrodes for high-performance supercapacitors. *J. Power Sources* **2017**, *352*, 34−41.
(2) Xiao, P.-W.; Meng, Q.; Zhao, L.; Li, J.-J.; Wei, Z.; Han, B.-H. Biomass-derived flexible porous carbon materials and their applications in supercapacitor and gas adsorption. *Mater. Des.* **2017**, *129*, 164−172.
(3) Neimark, A. V.; Ruetsch, S.; Kornev, K. G.; Ravikovitch, P. I.; Poulin, P.; Badaire, S.; Maugey, M. Hierarchical pore structure and wetting properties of single-wall carbon nanotube fibers. *Nano Lett.* **2003**, *3*, 419−423.
(4) Zhao, Y. L.; Liu, X. M.; Wang, J. J.; Zhang, S. J. Insight into the cosolvent effect of cellulose dissolution in imidazolium-based ionic liquid systems. *J. Phys. Chem. B* **2013**, *117*, 9042−9049.
(5) Qi, H. S.; Schulz, B.; Vad, T.; Liu, J. W.; Mäder, E.; Seide, G.; Gries, T. Novel carbon nanotube/cellulose composite fibers as multifunctional materials. *ACS Appl. Mater. Interfaces* **2015**, *7*, 22404−22412.
(6) Nguyen, D. D.; Tiwari, R. N.; Matsuoka, Y.; Hashimoto, G.; Rokuta, E.; Chen, Y.-Z.; Chueh, Y.-L.; Yoshimura, M. Low vacuum annealing of cellulose acetate on nickel towards transparent conductive CNT−graphene hybrid films. *ACS Appl. Mater. Interfaces* **2014**, *6*, 9071−9077.
(7) Zhu, C. C.; Chen, J. H.; Koziol, K. K.; Gilman, J. W.; Trulove, P. C.; Rahatekar, S. S. Effect of fibre spinning conditions on the electrical properties of cellulose and carbon nanotube composite fibres spun using ionic liquid as a benign solvent. *eXPRESS Polym. Lett.* **2014**, *8*, 154−163.
(8) Kafy, A.; Kim, H. C.; Yun, Y. M.; Kang, T. J.; Kim, J. Fabrication and characterization of cellulose nanofiber/graphene oxide blended fibers. *Proc. SPIE* **2018**, *10597*, 105970H.
(9) Kuzmenko, V.; Naboka, O.; Haque, M.; Staaf, H.; Göransson, G.; Gatenholm, P.; Enoksson, P. Sustainable carbon nanofibers/nanotubes composites from cellulose as electrodes for supercapacitors. *Energy* **2015**, *90*, 1490−1496.
(10) Kim, D.-H.; Park, S.-Y.; Kim, J.; Park, M. Preparation and properties of the single-walled carbon nanotube/cellulose nanocomposites using N-methylmorpholine-N-oxide monohydrate. *J. Appl. Polym. Sci.* **2010**, *117*, 3588−3594.
(11) Qi, H. S.; Liu, J. W.; Gao, S. L.; Mäder, E. Multifunctional films composed of carbon nanotubes and cellulose regenerated from alkaline/urea solution. *J. Mater. Chem. A* **2013**, *1*, 2161−2168.
(12) Zhu, S. D.; Wu, Y. X.; Chen, Q. M.; Yu, Z. N.; Wang, C. W.; Jin, S. W.; Ding, Y. G.; Wu, G. Dissolution of cellulose with ionic liquids and its application: a mini-review. *Green Chem.* **2006**, *8*, 325−327.
(13) Swatloski, R. P.; Spear, S. K.; Holbrey, J. D.; Rogers, R. D. Dissolution of cellulose with ionic liquids. *J. Am. Chem. Soc.* **2002**, *124*, 4974−4975.
(14) Sun, N.; Rahman, M.; Qin, Y.; Maxim, M. L.; Rodríguez, H.; Rogers, R. D. Complete dissolution and partial delignification of wood in the ionic liquid 1-ethyl-3-methylimidazolium acetate. *Green Chem.* **2009**, *11*, 646−655.
(15) Zavrel, M.; Bross, D.; Funke, M.; Büchs, J.; Spiess, A. C. High-throughput screening for ionic liquids dissolving (ligno-)cellulose. *Bioresour. Technol.* **2009**, *100*, 2580−2587.
(16) Ghamsari, A. K.; Wicker, S.; Woldesenbet, E. Bucky syntactic foam; multi-functional composite utilizing carbon nanotubes-ionic liquid hybrid. *Composites, Part B* **2014**, *67*, 1−8.
(17) Peng, R. G.; Wang, Y. Z.; Tang, W.; Yang, Y. K.; Xie, X. L. Progress in imidazolium ionic liquids assisted fabrication of carbon nanotube and graphene polymer composites. *Polymers* **2013**, *5*, 847−872.
(18) Bordes, E.; Morcos, B.; Bourgogne, D.; Andanson, J.-M.; Bussière, P.-O.; Santini, C. C.; Benayad, A.; Gomes, M. C.; Pádua, A. A. H. Dispersion and stabilization of exfoliated graphene in ionic liquids. *Front. Chem.* **2019**, *7*, 223.
(19) Javed, K.; Krumme, A.; Viirsalu, M.; Krasnou, I.; Plamus, T.; Vassiljeva, V.; Tarasova, E.; Savest, N.; Mere, A.; Mikli, V.; Danilson, M.; Kaljuvee, T.; Lange, S.; Yuan, Q.; Topham, P. D.; Chen, C.-M. A method for producing conductive graphene biopolymer nanofibrous fabrics by exploitation of an ionic liquid dispersant in electrospinning. *Carbon* **2018**, *140*, 148−156.
(20) Zhang, H.; Wang, Z. G.; Zhang, Z. N.; Wu, J.; Zhang, J.; He, J. S. Regenerated-cellulose/multiwalled-carbon-nanotube composite fibers with enhanced mechanical properties prepared with the ionic liquid 1-allyl-3-methylimidazolium chloride. *Adv. Mater.* **2007**, *19*, 698−704.
(21) Rahatekar, S. S.; Rasheed, A.; Jain, R.; Zammarano, M.; Koziol, K. K.; Windle, A. H.; Gilman, J. W.; Kumar, S. Solution spinning of cellulose carbon nanotube composites using room temperature ionic liquids. *Polymer* **2009**, *50*, 4577−4583.
(22) Lu, J.; Zhang, H. H.; Jian, Y. H.; Shao, H. L.; Hu, X. C. Properties and structure of MWNTs/cellulose composite fibers prepared by Lyocell process. *J. Appl. Polym. Sci.* **2012**, *123*, 956−961.
(23) Liu, Y. R. *Properties of ionic liquids for spinning of cellulose and recycling via freeze crystallization*; Technical University of Denmark, 2018.
(24) Sun, H.; You, X.; Deng, J.; Chen, X. L.; Yang, Z. B.; Ren, J.; Peng, H. S. Novel graphene/carbon nanotube composite fibers for efficient wire-shaped miniature energy devices. *Adv. Mater.* **2014**, *26*, 2868−2873.
(25) Liu, R.; Ma, L. N.; Huang, S.; Mei, J.; Li, E. Y.; Yuan, G. H. Large areal mass and high scalable and flexible cobalt oxide/graphene/bacterial cellulose electrode for supercapacitors. *J. Phys. Chem. C* **2016**, *120*, 28480−28488.
(26) Liu, Y.-R.; Thomsen, K.; Nie, Y.; Zhang, S.-J.; Meyer, A. S. Predictive screening of ionic liquids for dissolving cellulose and experimental verification. *Green Chem.* **2016**, *18*, 6246−6254.
(27) Liu, Y. R.; Meyer, A. S.; Nie, Y.; Zhang, S. J.; Zhao, Y. S.; Fosbøl, P. L.; Thomsen, K. Freezing point determination of water-ionic liquid mixtures. *J. Chem. Eng. Data* **2017**, *62*, 2374−2383.
(28) Hauru, L. K. J.; Hummel, M.; Michud, A.; Sixta, H. Dry jet-wet spinning of strong cellulose filaments from ionic liquid solution. *Cellulose* **2014**, *21*, 4471−4481.
(29) Luo, Z. Q.; Wang, A. Q.; Wang, C. Z.; Qin, W. C.; Zhao, N. N.; Song, H. Z.; Gao, J. G. Liquid crystalline phase behavior and fiber spinning of cellulose/ionic liquid/halloysite nanotubes dispersions. *J. Mater. Chem. A* **2014**, *2*, 7327−7336.
(30) Song, X.; Wang, C. W.; Xiao, S.; Zhang, X. Y.; Zhu, S. K.; Wang, Y.; Zhao, C. L. A method for testing the electrical conductivity of graphene powders. CN108458906A, 2018.
(31) Marinho, B.; Ghislandi, M.; Tkalya, E.; Koning, C. E.; de With, G. Electrical conductivity of compacts of graphene, multi-wall carbon nanotubes, carbon black, and graphite powder. *Powder Technol.* **2012**, *221*, 351−358.
(32) Härdelin, L.; Hagström, B. Wet spun fibers from solutions of cellulose in an ionic liquid with suspended carbon nanoparticles. *J. Appl. Polym. Sci.* **2015**, *132*, 41417.

DOI: 10.1021/acssuschemeng.9b05489
ACS Sustainable Chem. Eng. 2019, 7, 20013−20021

(33) Michardière, A.-S.; Mateo-Mateo, C.; Derré, A.; Correa-Duarte, M. A.; Mano, N.; Poulin, P. Carbon nanotube microfiber actuators with reduced stress relaxation. *J. Phys. Chem. C* **2016**, *120*, 6851−6858.
(34) Wang, W. J.; Nie, Y.; Liu, Y. R.; Bai, L.; Gao, J. S.; Zhang, S. J. Preparation of cellulose/multi-walled carbon nanotube composite membranes with enhanced conductive property regulated by ionic liquids. *Fibers Polym.* **2017**, *18*, 1780−1789.
(35) Yu, D. S.; Goh, K.; Wang, H.; Wei, L.; Jiang, W. C.; Zhang, Q.; Dai, L. M.; Chen, Y. Scalable synthesis of hierarchically structured carbon nanotube−graphene fibres for capacitive energy storage. *Nat. Nanotechnol.* **2014**, *9*, 555−562.
(36) Plimpton, S. Fast parallel algorithms for short-range molecular dynamics. *J. Comput. Phys.* **1995**, *117*, 1−19.
(37) Jorgensen, W. L.; Maxwell, D. S.; Tirado-Rives, J. Development and testing of the OPLS all-atom force field on conformational energetics and properties of organic liquids. *J. Am. Chem. Soc.* **1996**, *118*, 11225−11236.
(38) Wang, Y. L.; Qin, Z.; Buehler, M. J.; Xu, Z. P. Intercalated water layers promote thermal dissipation at bio−nano interfaces. *Nat. Commun.* **2016**, *7*, 12854.
(39) Liu, Z. P.; Chen, T.; Bell, A.; Smit, B. Improved united-atom force field for 1-alkyl-3-methylimidazolium chloride. *J. Phys. Chem. B* **2010**, *114*, 4572−4582.
(40) Giełdoń, A.; Bobrowski, M.; Bielicka-Giełdoń, A.; Czaplewski, C. Theoretical calculation of the physico-chemical properties of 1-butyl-4-methylpyridinium based ionic liquids. *J. Mol. Liq.* **2017**, *225*, 467−474.
(41) Wang, Y. L.; Wang, C. L.; Zhang, Y. Q.; Huo, F.; He, H. Y.; Zhang, S. J. Molecular insight on the regulatable interfacial property and flow behavior of confined ionic liquids in graphene nanochannels. *Small* **2019**, *15*, 1804508.
(42) Zhou, J.; Liu, X. M.; Zhang, S. J.; Zhang, X. P.; Yu, G. R. Effect of small amount of water on the dynamics properties and microstructures of ionic liquids. *AIChE J.* **2017**, *63*, 2248−2256.
(43) Li, C.; Zhao, Z. C.; Zhang, X. D.; Li, T. Y. Simulation and experimental study on thermal conductivity of [EMIM][DEP]+H2O +SWCNTs nanofluids as a new working pairs. *Int. J. Thermophys.* **2018**, *39*, 41−63.
(44) Hockney, R. W.; Eastwood, J. W. *Computer Simulation Using Particles*; Taylor & Francis, Inc.: Bristol, PA. 1988.
(45) Ebbesen, T. W.; Lezec, H. J.; Hiura, H.; Bennett, J. W.; Ghaemi, H. F.; Thio, T. Electrical conductivity of individual carbon nanotubes. *Nature* **1996**, *382*, 54−56.
(46) Salazar, P. F.; Chan, K. J.; Stephens, S. T.; Cola, B. A. Enhanced electrical conductivity of imidazolium-based ionic liquids mixed with carbon nanotubes: A spectroscopic study. *J. Electrochem. Soc.* **2014**, *161*, H481−H486.
(47) Krainoi, A.; Kummerlöwe, C.; Nakaramontri, Y.; Wisunthorn, S.; Vennemann, N.; Pichaiyut, S.; Kiatkamjornwong, S.; Nakason, C. Influence of carbon nanotube and ionic liquid on properties of natural rubber nanocomposites. *eXPRESS Polym. Lett.* **2019**, *13*, 327−348.
(48) Zhao, W.; Li, M.; Zhang, Z.; Peng, H. X. Carbon nanotube based composites film heater for de-icing application. *14th European Conference on Composite Materials*, Budapest, Hungary; ECCM, 2010; 545-ECCM14.
(49) Xu, Z. H.; Wei, C.; Gong, Y. Y.; Chen, Z. R.; Yang, D. J.; Su, H.; Liu, T. X. Efficient dispersion of carbon nanotube by synergistic effects of sisal cellulose nano-fiber and graphene oxide. *Compos. Interfaces* **2017**, *24*, 291−305.
(50) Ioniţă, M.; Crică, L. E.; Voicu, S. I.; Dinescu, S.; Miculescu, F.; Costache, M.; Iovu, H. Synergistic effect of carbon nanotubes and graphene for high performance cellulose acetate membranes in biomedical applications. *Carbohydr. Polym.* **2018**, *183*, 50−61.
(51) Jing, L.; Li, H. L.; Lin, J. J.; Tay, R. Y.; Tsang, S. H.; Teo, E. H. T.; Tok, A. I. Y. Supercompressible coaxial carbon nanotube@graphene arrays with invariant viscoelasticity over − 100 to 500 °C in ambient air. *ACS Appl. Mater. Interfaces* **2018**, *10*, 9688−9695.
(52) Dichiara, A. B.; Song, A.; Goodman, S. M.; He, D.; Bai, J. Smart papers comprising carbon nanotubes and cellulose microfibers for multifunctional sensing applications. *J. Mater. Chem. A* **2017**, *5*, 20161−20169.
(53) Ramesh, S.; Khandelwal, S.; Rhee, K. Y.; Hui, D. Synergistic effect of reduced graphene oxide, CNT and metal oxides on cellulose matrix for supercapacitor applications. *Composites, Part B* **2018**, *138*, 45−54.
(54) Lin, J.; Zhang, C. G.; Yan, Z.; Zhu, Y.; Peng, Z. W.; Hauge, R. H.; Natelson, D.; Tour, J. M. 3-dimensional graphene carbon nanotube carpet-based microsupercapacitors with high electrochemical performance. *Nano Lett.* **2013**, *13*, 72−78.
(55) Zhao, X. Y.; Lu, X.; Tze, W. T. Y.; Wang, P. A single carbon fiber microelectrode with branching carbon nanotubes for bioelectrochemical processes. *Biosens. Bioelectron.* **2010**, *25*, 2343−2350.
(56) Chen, X. L.; Qiu, L. B.; Ren, J.; Guan, G. Z.; Lin, H. J.; Zhang, Z. T.; Chen, P. N.; Wang, Y. G.; Peng, H. S. Novel electric double-layer capacitor with a coaxial fiber structure. *Adv. Mater.* **2013**, *25*, 6436−6441.
(57) Atif, R.; Inam, F. Reasons and remedies for the agglomeration of multilayered graphene and carbon nanotubes in polymers. *Beilstein J. Nanotechnol.* **2016**, *7*, 1174−1196.

DOI: 10.1021/acssuschemeng.9b05489
ACS Sustainable Chem. Eng. 2019, 7, 20013−20021